

Exergy Based Performance Analysis of a Solid Adsorption Solar Refrigerator

N. V. Ogueke*[‡], C. Ndeke*, E. E. Anyanwu*

*Mechanical Engineering Department Federal University of Technology PMB 1526, Owerri.

(nvogueke@futo.edu.ng, chyndekebuike@yahoo.co.uk, eemmanuelanyanwu@yahoo.com)

[‡]Corresponding Author; N. V. Ogueke, +234 805 300 6458, nvogueke@futo.edu.ng

Received: 20.03.2014 Accepted: 02.05.2014

Abstract- The exergy based performance analysis of a solid adsorption solar refrigerator is presented. The analysis is based on an exergy balance applied to each component of the refrigeration machine, leading to a general exergy balance equation. The dead state temperature was chosen to coincide with the ambient temperature. Results reveal that maximum exergy destruction occurred in the collector/generator/adsorber during heat up and adsorbate desorption phases with a value of 3747.77 kJ. Values recorded in the condenser and evaporator were 10.51 and 20.11 kJ, respectively while the exergy efficiency was in the range of 0.0008 – 0.012. It was also found that the rate of exergy destruction reduced as soon as adsorbate generation commenced; indicating superior energy and exergy utilization during desorption phase. Thus use of adsorbent and adsorbate with the potential of very early commencement of desorption can significantly improve the exergetic efficiency of the system.

Keywords- Exergy, Solar, Adsorption, Refrigerator.

1. Introduction

Cold is one of the major necessities of life. It is primarily employed in the preservation of agricultural produce, vaccines and for provision of comfort in homes and offices. Until recently, the vapour compression refrigeration system powered by electrical energy derived mostly from fossil fuels has been the major source of cold production. Unfortunately this system of cold production has been variously implicated in the damage of our environment chiefly through attack on the ozone layer, by the refrigerants used, and global warming because of the high carbon footprint associated with its operation. This is basically responsible for the growing interest in the heat operated counterparts. The beauty of the heat operated systems is that they can be powered by low grade heat like solar and biomass. They also have little or no moving parts and the refrigerants employed are environmentally friendly. Thus they have simpler controls, operate more quietly and have lower operating cost. When the energy source is solar, the only cost associated with it is the cost of the solar energy harvesting equipment (Anyanwu et al, 2001).

Heat operated refrigerators are basically of two types; absorption and adsorption systems. Solid adsorption solar

refrigerator is one of these two, with one complete cycle of operation occurs in 24 hours. This comprises the diurnal phase which consists of the heat up, desorption and cool-down phases and the nocturnal phase which covers the adsorbate evaporation and re-adsorption phases. The major components of a typical solid adsorption solar refrigerator are: the collector/generator/adsorber, the condenser and the evaporator. Several authors have reported successful cold production using this refrigeration system. They include the works of Critoph (1994) using activated carbon/ammonia working pair, Anyanwu and Ezekwe (2003) using activated carbon/methanol working pair; Hildbrand et al (2004) using Silica-gel/Water working pair, Li et al (2004) using Activated Carbon/Ethanol, Lemmini and Errougani (2005) using Activated Carbon/Methanol and Wang et al. (2011) using Activated Carbon/Ammonia. One conclusion general to all is their low COP.

Many numerical and thermodynamic studies of the cooling system have been undertaken with the aim of optimizing its performance. Hassan et al (2011) numerically studied an adsorption refrigerator using activated carbon/methanol adsorbent/adsorbate pair. The study took into account the variations of ambient temperature and solar radiation during the day. In addition, they investigated the

local pressure and local thermal conductivity variations in space and time inside the reactor. Their result showed that a COP of 0.211 was possible. Similarly, Zhao et al (2011) used an experimental data to validate their dynamic mathematical model developed using a non-uniform pressure assumption and the introduction of a transient boundary condition of the diffusion equation. Their results revealed that the transient boundary condition improved accuracy of the model and was capable of reflecting the dynamic shift of dominant driving forces from diffusion driving to temperature driving. Li and Wang (2003) developed a uniform pressure model describing the heat and mass transfer in the adsorbent bed for a flat plate solar ice maker. The numerical result showed that the model predicted the dynamic response of the solid adsorption solar refrigerator to about 4% accuracy. Thus, they concluded that the model was a good optimization tool for the solar refrigerator. Ogueke and Anyanwu (2008) worked on the design improvement of a collector/generator/adsorber of a solid adsorption solar refrigerator and concluded that an improvement in COP of 29 – 38% is possible with optimal choices of tube spacing, adsorbent packing density and collector plate/adsorbent tube material combinations. Jing and Exell (1994) carried out the simulation and sensitivity analysis of an intermittent solar-powered charcoal/methanol refrigerator and found out that the efficiency the collector/generator/adsorber increases with increase in daily insolation while there appears to be an optimum outside diameter for the collector tube, which is dependent on the local meteorological conditions.

Anyanwu and Ogueke (2005) used the second law of thermodynamics to propose a thermodynamic based design procedure for the solid adsorption solar refrigerator while Pon et al (1999) proposed a second law of thermodynamics based figure of merit for comparing the performances of sorption systems for cooling and heat pump application. Unfortunately, these approaches do not give quantitative and qualitative assessment of the various losses occurring in the various components of the system, and by extension, the entire refrigerator. This explains why emphasis is shifting towards exergy based system performance analysis.

Exergy analysis provides a clear distinction between the energy losses to the environment and internal irreversibility in the process (Baiju and Muraleedharan, 2012). Thus, it is possible to determine the most critical component with respect to efficient energy utilization. Authors, (Baiju and Muraleedharan, 2012; Vasilescu et al, 2007; Baiju and Muraleedharan, 2013 and You et al, 2000), have reported analysis of the adsorption refrigeration using this approach. However, most of the physical systems used are laboratory models. Even when the tests done for the systems studied were under the climatic condition of the location, the exergy analysis concentrated on the total exergy destruction of its individual components and the variation of exergy destruction with the generator temperature. No study of the system, detailing how exergy destruction varied as it undergoes a complete cycle of operation, has been presented. Such treatment will provide insight into the irreversibility trend of the adsorption solar refrigerator as it undergoes its complete cycle of operation. Furthermore, a single dead state temperature was adopted for the analysis so far presented in

spite of the fact that physical systems interact directly with the ambient environment. Therefore, the use of a single dead state temperature may not be a true representation of the actual interaction between the components of the refrigerator and the ambient environment, since the ambient temperature changes throughout during one complete cycle of refrigerator operation.

Consequently, in this work, we present an exergy based performance analysis of a physical system installed and tested under the meteorological conditions of Nsukka, Nigeria. The dead state temperature adopted coincides with the location ambient temperature.

2. Methodology

2.1. The Solid Adsorption Solar Refrigerator

Figure 1 show the solid adsorption refrigerator studied. It consists of the collector/generator/adsorber, the condenser, a liquid receiver and an evaporator. The refrigerator operates intermittently in a cycle which comprises the heat-up, desorption, cool-down and refrigeration phases as shown in the Pressure-Temperature-Concentration (PTX) diagram of Figure 2. During the heat-up phase (process 1-2), solar radiation captured results in the sensible heating of the adsorbent from ambient temperature resulting in pressure increase in the collector/generator/adsorber. As the heating continues, a pressure value is attained which equals the saturation vapour pressure corresponding to the condenser temperature (state 2). This indicates the commencement of desorption phase (process 2-3) and the collector/generator/adsorber at this stage is linked to the condenser.

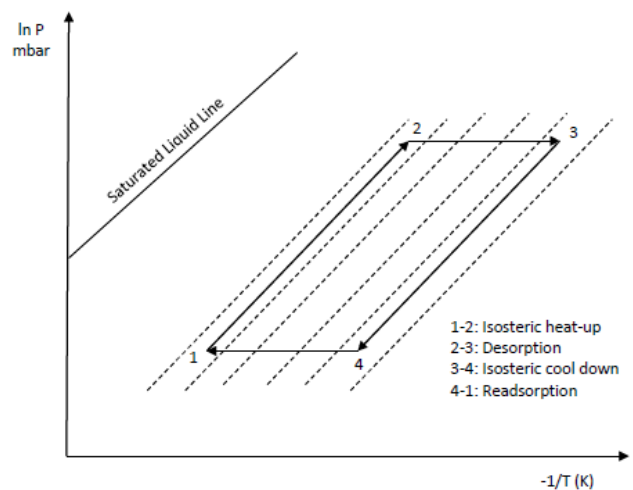


Fig. 1. P-T-X Diagram of a typical adsorption cycle.

Desorption phase occurs at a relatively constant temperature and it is marked by the release of the adsorbed adsorbate and its subsequent conversion to liquid in the condenser. At the end of desorption phase (state 3), the condenser is isolated from the collector/generator/adsorber which is then allowed to cool. This is the cool-down (process 3-4) phase and it is accompanied by pressure drop. When this pressure equals the saturation pressure corresponding to the

evaporator pressure (state 4), the collector/generator/adsorber is linked to the evaporator thus marking the commencement of the refrigeration phase (process 4-1). At this phase, the adsorbate earlier condensed is evaporated and re-adsorbed by the adsorbent while producing cooling in the process. More detailed description of the refrigerator's components, the mode of operation as well as the specifications and some of the results obtained are contained in Anyanwu and Ezekwe (2003) and Anyanwu and Ogueke (2007).

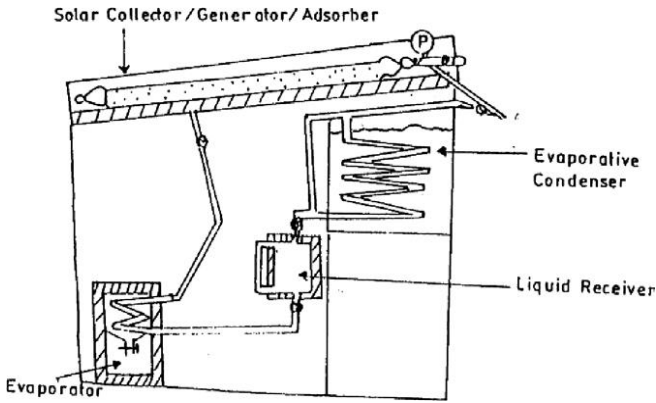


Fig. 2. Schematic diagram of the solid adsorption solar refrigerator.

2.2. The Exergy Analysis

Exergy analysis of the system will require applying an exergy balance to each of the components of the refrigerator under study to obtain its general exergy balance equation. However Vasilescu et al (2007) gave the general exergy balance equation as in eqn. (1).

$$\Delta U - T_0 \Delta S = \sum \left(1 - \frac{T_0}{T} \right) Q + \sum_i m(h - T_0 s) - \sum_f m(h - T_0 s) - T_0 \Delta S_g \quad (1)$$

The quantity $\Delta U - T_0 \Delta S$ is the maximum work potential and $T_0 \Delta S_g = \Pi$ is the exergy destroyed, according to Gouy-Stodola theorem, during the closed flow process. The summation $\sum \left(1 - \frac{T_0}{T} \right) Q = \sum ExQ$ denotes heat exergy while $\sum_i m(h - T_0 s) - \sum_f m(h - T_0 s) = \sum \varepsilon_i - \sum \varepsilon_f$ is the variation of the mass exergy between the entrance to and exit from the system. ΔU is change in internal energy of the process being considered and T_0 is the dead state reference temperature. ΔS is the entropy change in the process. Rearranging eqn. (1) in terms of the exergy destroyed gives:

$$\Pi = \sum ExQ + \sum \varepsilon_i - \sum \varepsilon_f - (\Delta U - T_0 \Delta S) \quad (2)$$

A Complete cycle of the adsorption refrigerator considered consists of the following four phases: isosteric heat-up, desorption, isosteric cool-down and re-adsorption.

Eqn. (2) is therefore applied to each of the phases, putting into consideration its peculiarities.

From the first law of thermodynamics

$$dU = dQ + dW \quad (3)$$

The containment vessel of the generator/adsorber does not move under pressure. Thus $dW = 0$. Therefore,

$$dU = dQ \quad (4)$$

2.2.1. Isosteric heat-up phase

During this phase (process 1-2 in Figure 2), the collector/generator/adsorber is sensibly heated at constant adsorbate mass. Thus $\sum \varepsilon_i - \sum \varepsilon_f = 0$ and eqn. (2) reduces to

$$\Pi_{12} = \sum Ex(Q_{12}) - (\Delta U - T_0 \Delta S) \quad (5)$$

where,

$$Ex(Q_{12}) = \left(1 - \frac{T_0}{T_{com}} \right) \left(\int_{T_1}^{T_2} m_a c_{pa} dT + \int_{T_1}^{T_2} m_{r,i} c_{pr} dT \right) \quad (6)$$

The change in internal energy is obtained from

$$\Delta U_{12} = \left(\int_{T_1}^{T_2} m_a c_{pa} dT + \int_{T_1}^{T_2} m_{r,i} c_{pr} dT \right) \quad (7)$$

while the entropy change is given by eqn. (8)

$$\Delta S_{12} = \left(\int_{T_1}^{T_2} m_a c_{pa} \frac{dT}{T} + \int_{T_1}^{T_2} m_{r,i} c_{pr} \frac{dT}{T} \right) \quad (8)$$

2.2.2. Desorption phase

This phase is represented by process 2-3 in Figure 2 and it is characterised by adsorbate generation. Heat added to the collector/generator/adsorber is partly used in adsorbate generation and partly produces sensible heating of the collector/generator/adsorber. Consequently the exergy loss is given by:

$$\Pi_{23} = \sum Ex(Q_{23}) + \sum \varepsilon_i - \sum \varepsilon_f - (\Delta U_{23} - T_0 \Delta S_{23}) \quad (9)$$

where,

$$Ex(Q_{23}) = \left(1 - \frac{T_0}{T_{com}} \right) \left\{ \left(\int_{T_2}^{T_3} m_a c_{pa} dT + \int_{T_2}^{T_3} (m_{r,i} - m_{r,g}) c_{pr} dT \right) + m_{r,g} \Delta h_{23} + m_{r,g} h_{sg} \right\} \quad (10)$$

The variation of mass exergy, changes in internal energy and entropy are obtained from eqns 11, 12 and 13, respectively.

$$\varepsilon_f - \varepsilon_i = m_{r,g} \left(h_{sg} - T_0 \frac{h_{sg}}{T_{com}} \right) \quad (11)$$

$$\Delta U_{23} = \left(\int_{T_2}^{T_3} m_a c_{pa} dT + \int_{T_2}^{T_3} (m_{r,i} - m_{r,g}) c_{pr} dT \right) + m_{r,g} \Delta h_{23} + m_{r,g} h_{sg} \quad (12)$$

$$\Delta S_{23} = \left(\int_{T_2}^{T_3} m_a c_{pa} \frac{dT}{T} + \int_{T_2}^{T_3} (m_{r,i} - m_{r,g}) c_{pr} \frac{dT}{T} + \frac{m_{r,g} \Delta h_{23}}{T} + \frac{m_{r,g} h_{sg}}{T} \right) \quad (13)$$

2.2.3. *Isosteric cool-down phase*

This phase is shown as process 3-4 in Figure 2. During this process, the mass of refrigerant in the collector/generator/adsorber remains constant as it cools to the dead state temperature, T_0 . Thus $\sum \varepsilon_i - \sum \varepsilon_f = 0$ and the exergy loss becomes

$$\Pi_{34} = \sum Ex(Q_{34}) - (\Delta U_{34} - T_0 \Delta S_{34}) \quad (14)$$

where the heat exergy is given by:

$$Ex(Q_{34}) = \left(1 - \frac{T_0}{T_{com}} \right) Q_{34} = 0 \quad (15)$$

$$\Delta U_{34} = \left(\int_{T_3}^{T_4} m_a c_{pa} dT + \int_{T_3}^{T_4} (m_{r,i} - m_{r,g}) c_{pr} dT \right) \quad (16)$$

$$\Delta S_{34} = \left(\int_{T_3}^{T_4} m_a c_{pa} \frac{dT}{T} + \int_{T_3}^{T_4} (m_{r,i} - m_{r,g}) c_{pr} \frac{dT}{T} \right) \quad (17)$$

2.2.4. *Re-adsorption phase*

During this phase (process 4-1 in Figure 2), the refrigerant evaporated at the evaporator is re-adsorbed in the collector/generator/adsorber. There is therefore an increase in adsorbate mass; hence the exergy loss is obtained from

$$\Pi_{41} = \sum Ex(Q_{41}) + \sum \varepsilon_i - \sum \varepsilon_f - (\Delta U_{41} - T_0 \Delta S_{41}) \quad (18)$$

The heat exergy and variation in mass exergy are given by eqns. 19 and 20, respectively.

$$Ex(Q_{41}) = \left(1 - \frac{T_0}{T_{com}} \right) Q_{41} = 0 \quad (19)$$

$$\varepsilon_f - \varepsilon_i = -m_{r,a} \left(h_{sg} - T_0 \frac{h_{sg}}{T_{com}} \right) \quad (20)$$

The internal energy change is computed from eqn. (21) and the entropy change from eqn. (22).

$$\Delta U_{41} = \left(\int_{T_3}^{T_4} m_a c_{pa} dT + \int_{T_3}^{T_4} (m_{r,i} - m_{r,g} + m_{r,ad}) c_{pr} dT \right) \quad (21)$$

(21)

$$\Delta S_{41} = \left(\int_{T_3}^{T_4} m_a c_{pa} \frac{dT}{T} + \int_{T_3}^{T_4} (m_{r,i} - m_{r,g} + m_{r,ad}) c_{pr} \frac{dT}{T} + \frac{m_{r,a} h_{sg}}{T} \right) \quad (22)$$

2.2.5. *The Condenser*

In the condenser, the desorbed adsorbate loses heat, equivalent to its latent heat of vaporization, and changes to liquid. Its flow velocity as the heat exchange takes place is very low. Thus a quasi-stationary operation regime is assumed without internal energy and entropy generation as in Vasilescu et al (2007). Furthermore, it is assumed that no condensate subcooling occurs. Hence the exergy destruction becomes:

$$\Pi_{cd} = Ex(Q_{cd}) - (\varepsilon_f - \varepsilon_i) \quad (23)$$

Where the heat exergy is given as:

$$Ex(Q_{cd}) = \left(1 - \frac{T_0}{T_{cd}} \right) Q_{cd} \quad (24)$$

The quantity of heat given out during the phase change process is obtained from

$$Q_{cd} = m_{r,g} L_e \quad (25)$$

while the mass exergy variation is given by:

$$(\varepsilon_f - \varepsilon_i) = m_{r,g} \left(L_e - T_0 \frac{L_e}{T_{cd}} \right) \quad (26)$$

T_{cd} is related to the ambient temperature by the expression for an evaporative condenser given in Anyanwu and Ogueke (2005) as

$$T_{cd} = 159.6 + 0.4574 T_{am} \quad (27)$$

2.2.6. *The Evaporator*

In the evaporator, the adsorbate generated evaporates thus producing cooling. Mass flow rate of liquid adsorbate in the evaporator, as well as that of vapour produced due to the evaporation process is generally low, thus a quasi-stationary operation regime, as in section 3.5, is assumed. Also assumed is that superheating of adsorbate does not occur. Therefore the exergy destruction becomes:

$$\Pi_{ev} = Ex(Q_{ev}) - (\varepsilon_f - \varepsilon_i) \quad (28)$$

and the heat exergy is given as:

$$Ex(Q_{ev}) = \left(1 - \frac{T_0}{T_{ev}}\right) Q_{ev} \quad (29)$$

The quantity of heat extracted by the evaporating adsorbate is obtained from

$$Q_{ev} = m_{r,e} L_e \quad (30)$$

while the mass exergy variation is obtained from eqn. (31).

$$(\varepsilon_f - \varepsilon_i) = m_{r,e} \left(L_e - \frac{L_e}{T_{ev}} \right) \quad (31)$$

2.2.7. Exergy efficiency

The exergy efficiency is defined as the ratio of exergy output in the system to the exergy input. Mathematically,

$$\psi_{ex} = \frac{|Ex(Q_{ev})|}{Ex(Q_{des})} \quad (32)$$

Where

$$Ex(Q_{des}) = |Ex(Q_{ev})| + \Pi \quad (33)$$

and

$$\Pi = \Pi_{12} + \Pi_{23} + \Pi_{34} + \Pi_{41} + \Pi_{cd} + \Pi_{ev} \quad (34)$$

while

$$Ex(Q_{des}) = Ex(Q_{12}) + Ex(Q_{23}) \quad (35)$$

3. Results and Discussion

Figures 3 – 5 show the exergy destroyed in the generator, condenser and evaporator during one complete cycle of operation. This result reveals that the highest exergy destruction occurs in the generator during the heat-up and desorption phases.

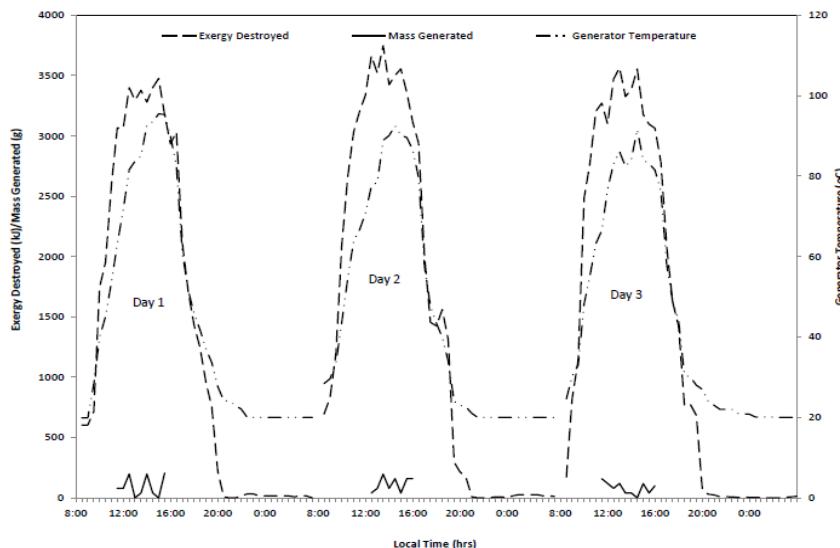


Fig. 3. Exergy destruction in the generator during one complete cycle for three different days.

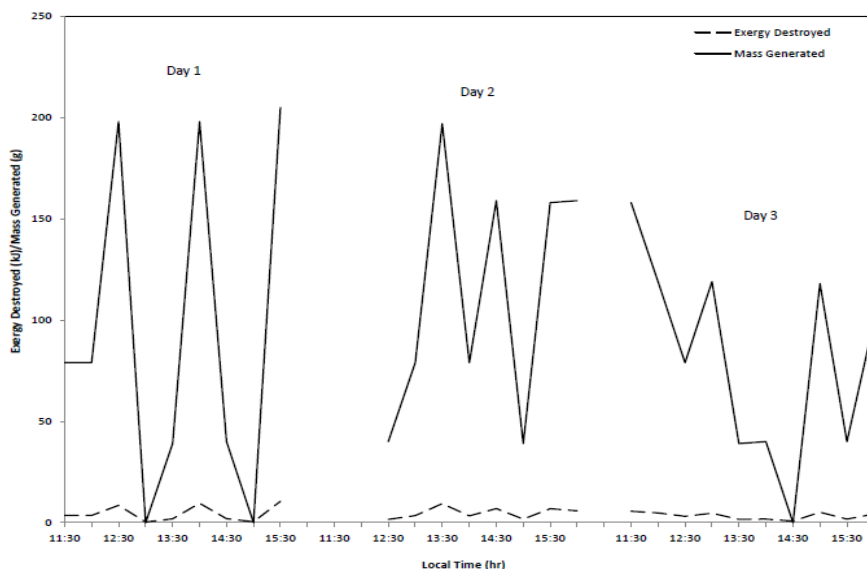


Fig. 4. Exergy destruction in the condenser for the three days considered.

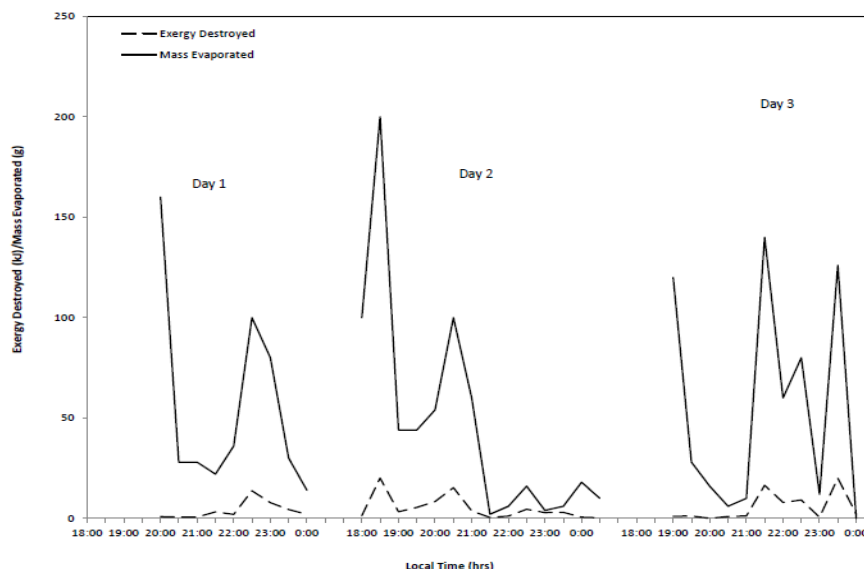


Fig. 5. Exergy destruction in the evaporator for the days considered.

The exergy destruction initially increases with time as the generator is heated. However with the outset of adsorbate generation, the rate of increase in exergy destruction begins to slow down and subsequently, exergy destruction starts reducing. This reduction in exergy destruction continues until adsorbate generation ceases. Ordinarily, exergy destruction is expected to increase with the generator temperature. This was the trend until desorption commenced. Subsequently the rate of increase in exergy destruction depended more on the mass of adsorbate generated than the increase in the generator temperature. This is seen from Fig. 3 where it is shown that once desorption is in progress, increased generator temperature did not necessarily lead to increased exergy loss. For instance between 11:30 and 15:30 hrs on day 1, when adsorbate generation was in progress, the adsorbate temperature increased from 71 – 95°C while the exergy destruction fluctuated between 2932 – 3476 kJ with a profile mimicking that of the adsorbate generation. This was also the case on days 2 and 3 during desorption phase. However before the commencement of the desorption phase,

say between 8:00 – 11:30 hrs on day 1, the adsorbate temperature increased from about 20 – 63°C and the exergy destruction increased steadily from 603 – 3065 kJ.

This behaviour may be attributed to the increased exergy consumption associated with the desorption process. Increased temperature leads to increase in entropy generation and subsequently an increased irreversibility and exergy destruction. However adsorbate generation is an endothermic process. Its utilization of the heat energy, for adsorbate generation, which would have resulted in increased entropy results in a reduction in the attendant exergy loss. The highest exergy destruction observed for the generator implies that it is the most critical component of the solid adsorption refrigerator when it comes to improving its performance. Furthermore since adsorbate desorption reduces exergy destruction, the use of adsorbent and adsorbate with the potential of very early commencement of desorption can significantly improve the exergetic efficiency of the system. At present, adsorbent/adsorbate combinations used in adsorption refrigeration do not have this quality. Thus further

performance improvement research may be channelled towards this.

The highest recorded exergy destruction at the condenser was 10.51 kJ, and this occurred in day 1. This value is very low compared to the recorded values in the generator as shown in the figures. Within the condenser the major source of irreversibility is the phase change process leading to condensation. This is more evident from Figure 4 where it is shown that exergy destroyed depended on mass of adsorbate desorbed. With more adsorbate desorbed, the heat transfer needed for desorption to increase thus leading to increase in exergy destruction. Similarly in the evaporator, exergy destruction is mainly due to the irreversible phase change which produces cooling. Figure 5 shows the dependence of exergy destruction on mass of adsorbate evaporated and further reveals a highest exergy destruction of 20.11 kJ. The maximum values of 10.51 and 20.11 kJ recorded for the

condenser and evaporator, respectively, when compared with a value of 3747.77 kJ obtained for the generator reveals how low the performance improvement of solid adsorption refrigerator depends on the condenser and evaporator.

Figure 6 shows the refrigerator exergy efficiency from the commencement of evaporation process to the end of the evaporation process or when no further cooling was recorded in the evaporator. This figure reveals that at the end of each day's cooling, the exergy efficiency was between 0.0008 – 0.012. These values are quite low compared to the COP values of 0.056 – 0.093 reported for the same system by Anyanwu and Ezekwe (2003). Considering that the generator performance greatly influences the overall system performance, this low exergy efficiency may be associated with the low collector efficiency of 11.6 – 16.4% recorded for the collector/generator/adsorber of the said system.

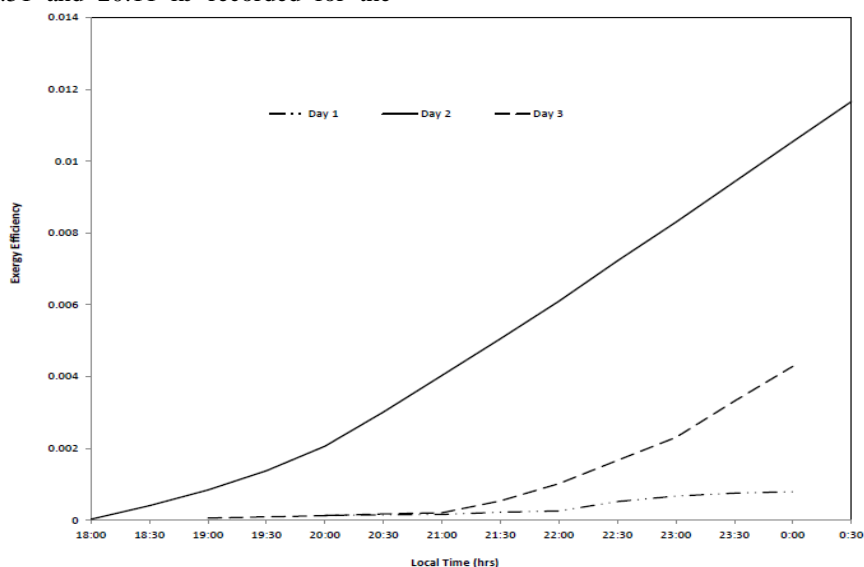


Fig. 6. Variation of exergy efficiency as cooling progressed.

4. Conclusion

The exergy based performance analysis of a solid adsorption solar refrigerator has been presented. The analysis which considered how exergy destruction varied as the refrigerator undergoes one complete cycle revealed that:

- i. Exergy destruction is highest in the collector/generator/adsorber and this occurs during the isosteric heat-up and desorption phases.
- ii. The rate of increase of exergy destruction begins to decrease with the outset of adsorbate desorption; thus leading to exergy destroyed not necessarily increasing with an increase in the collector/generator/adsorber temperature. This is an indication that energy is more usefully utilized during this process.
- iii. The exergy efficiency of the system is low; the range being 0.0008 – 0.012 compared to an experimental COP of 0.056 – 0.093 obtained for the same system.
- iv. Exergy destruction reduction and subsequently an overall increase in the exergy efficiency can be

achieved by using an adsorbate with much lower saturation temperature at the prevailing condensing temperatures in combination with an adsorbent which begins desorbing at lower temperatures.

References

- [1] C. Hilbrand, D. Philippe, M. Pons and F. Buchter, "A new solar powered adsorption refrigerator with high performance. *Solar Energy*, vol. 77, No. 3, pp. 311 – 318, 2004.
- [2] E. E. Anyanwu and C. I. Ezekwe, "Design, construction and test run of a solid adsorption solar refrigerator using activated carbon/methanol as adsorbent/adsorbate pair", *Energy Conversion and Management*, vol. 44, pp. 2879 – 2892, 2003.
- [3] E. E. Anyanwu and N. V. Ogueke, "Thermodynamic Design Procedure for Solid Adsorption Solar Refrigerator", *Renewable Energy*, vol. 30, pp. 81 – 96, 2005.

- [4] E. E. Anyanwu and N. V. Ogueke, "Transient Analysis and Performance Prediction of a Solid Adsorption Solar Refrigerator", *Applied Thermal Engineering*, vol. 27, pp. 2514 – 2523, 2007.
- [5] E. E. Anyanwu, U. U. Oteh and N. V. Ogueke, "Simulation of a solid adsorption solar refrigerator using activated carbon/methanol adsorbent/adsorbate pair", *Energy Conversion and Management*, vol. 42, pp. 899 – 915, 2001.
- [6] E. E. Vasilescu, R. Boussehain, M. Feidt, and A. Dobrovicescu, "Energy and exergy optimization of the adsorption refrigeration machine with simple and double effect", *TERMOTEHNICA*, vol.1- 2, pp. 80 – 86, 2007.
- [7] F. Lemmini and A. Errougani, "(2005). Building and experimentation of a solar powered adsorption refrigerator", *Renewable Energy*, vol. 30, pp. 1989 – 2003, 2005.
- [8] H. Z. Hassan, A. A. Mohamad and R. Bennacer, "Simulation of an adsorption solar cooling system", *Energy*, vol. 36, No. 1, pp. 530 – 537, 2011.
- [9] Hu, Jing and R. H. B. Exell, "Simulation and sensitivity analysis of intermittent solar powered charcoal/methanol refrigeration" *Renewable Energy*, vol. 4, No. 1, pp. 133 – 149, 1994.
- [10] I. Dincer and A. R. Marc, *Exergy, Energy, Environment and Sustainable Development*, 2nd Ed., Oxford:Elsevier Ltd., 2013.
- [11] Li, M. and Wang, R.Z. (2003). Heat and mass transfer in a flat plate solar solid adsorption refrigeration ice maker. *Renewable Energy*, 28 (4), pp. 613 – 622.
- [12] M. Li, M. B. Huang, H. B. R. Z. Wang, L. L. Cai, W.D. and Yang, W.M. (2004). Experimental study on adsorbent of activated carbon with refrigerant of methanol and ethanol for solar ice maker. *Renewable Energy*, 29, pp. 2235 – 2244.
- [13] M. Pons, F. Meunier, G. Cacciola, R. E. Critoph, M. Groll, L. Puigjaner, B. Spinner and F. Ziegler, "Thermodynamic based comparison of sorption systems for cooling and heat pumping", *International Journal of Refrigeration*, vol. 22, pp. 5 – 17, 1999.
- [14] N. V. Ogueke and E. E. Anyanwu, "Design improvements for a collector/generator/adsorber of a solid adsorption solar refrigerator", *Renewable Energy*, vol. 33, pp. 2428 – 2440, 2008.
- [15] R. E. Critoph, "An ammonia carbon solar refrigerator for vaccine cooling", *Renewable Energy*, vol. 5, No(1 – 4), pp. 502 – 508, 1994.
- [16] R. Z. Wang, Z. Z. Xia, L. W. Wang, Z. S. Lu, S. L. Li, T. X. Li, J. Y. Wu, and S. He, "Heat transfer design in adsorption refrigeration systems for efficient use of low-grade thermal energy", *Energy*, vol. 36, No. 9, pp. 5425 – 5439, 2011.
- [17] V. Baiju and C. Muraleedharan, "Exergy Assessment of Single Stage Solar Adsorption Refrigeration System Using ANN", *International Scholarly Research Network Mechanical Engineering*, pp. 1 – 10, 2012.
- [18] V. Baiju and C. Muraleedharan, "Energy and exergy analysis of solar hybrid adsorption refrigeration system", *International Journal of Sustainable Engineering*, vol. 6, No. 4, pp. 289 – 300, 2013.
- [19] Y. L. Zhao, E. Hu and A. Blazewicz, "A non-uniform pressure and transient boundary condition based dynamic modeling of the adsorption process of an adsorption refrigeration tube", *Applied Energy*, vol. 90, No. 1, pp. 280 – 287, 2012.
- [20] Y. You, E. Hu and J. Jarvis, "The Exergy (Availability) Analysis on the Solar Adsorption Refrigeration System Working around the Atmospheric Pressure" In David Mills, John M. Bell, Stoykov LA and Prasad KDV Yarlagadda (eds), *SOLAR 2000. Proceedings of the 38th Annual Conference of the Australian and New Zealand Solar Energy Society*, Brisbane, Australia. pp. 340 – 347.